Journal of Materials Chemistry A

Accepted Manuscript

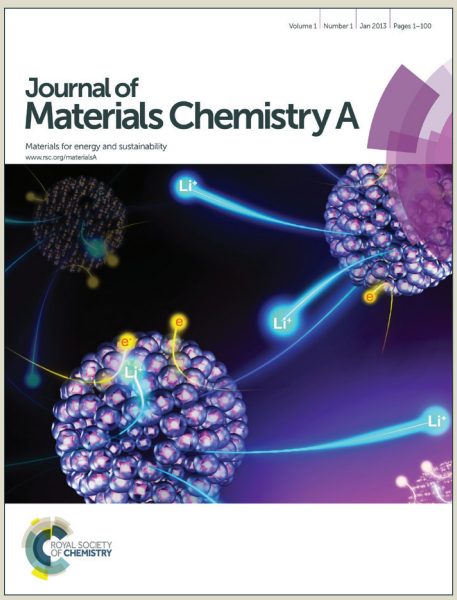

ROYAL SOCIETY OF CHEMISTRY

www.rsc.org/materialsA

Self-supported carbon coated TiN nanotube arrays: Innovative carbon coating leads to improved cycling ability for supercapacitor applications

*Fabian Grote, Huaping Zhao, and Yong Lei**[1]

Ilmenau University of Technology, Institute of Physics and IMN MacroNano® (ZIK), Prof. Schmidt Str. 26, 98693 Ilmenau, Germany

Self-supported carbon coated TiN nanotube arrays are synthesized by an innovative conformal carbon coating technique based on a self-assembly approach of polymeric nano-micelles on nano-porous anodic aluminum oxide templates and a straight forward atomic layer deposition process to fabricate TiN. Unlike most reported, the functional carbon coating is prepared first in this attempt. Then, the active electrode material is deposited inside, guaranteeing a highly conformal coating and a well control of the structural parameters, all combined with the self-supporting nature of the nanostructure array. The synthesized carbon coated TiN nanotube arrays are tested as a negative electrode material for aqueous based supercapacitor devices. It is shown that the functional carbon coating is leading to an improved long-term cycling ability compared to bare TiN nanotube arrays.

[1] e−mail: yong.lei@tu-ilmenau.de, tel.: +49 3677 69-3748

1. Introduction

Carbon coatings on functional nanomaterials have attracted much attention in nanotechnology. In particular, energy related applications, such as solar water splitting, Li-ion batteries, and supercapacitors can strongly benefit from carbon coatings.[1-4] Up to now, nanostructured materials are commonly carbon coated by techniques such as chemical and physical vapor deposition, and hydrothermal glucose coating with subsequent carbonization.[4, 5] Unfortunately, all available techniques prepare the carbon coating after the synthesis of the active material, which may lead to a poor structural controllability, non-conformal coating, and collapse of the nanostructured material during high temperature carbonization processes. Importantly, such approaches were initially developed for thin films and powder samples and are not capable of coating self-supported 3D dense nanostructure arrays in a conformal manner, but in particular such arrays are widely believed among scientist to strongly enhance the performance of the as-mentioned applications.[6-10] As a cost-effective approach to fabricate large-scale, dense, and highly defined 3D nanostructure arrays, nano-porous anodic aluminum oxide (AAO), a self-organized high aspect ratio nanomaterial that can be synthesized by a straight forward anodization process from aluminum, has been extensively applied as a template to synthesis self-supported nanostructures for a wide range of applications.[11-14] However, a successful technique to synthesize conformal carbon coatings on AAO prepared self-supported nanostructure arrays has not, to our knowledge, been previously reported. The fabrication of a conformal functional carbon coating inside an AAO template prior to the active material deposition could circumvent the as-described limitations.

By combining well established AAO technology with an innovative carbon coating technique, which is based on the self-assembly of polymeric nano-micelles (PNMs) on the AAO template,

we could developed a versatile approach that is capable of first synthesizing the functional carbon coating within the AAO pores and subsequently depositing the active material inside by utilizing a straight forward atomic layer deposition (ALD) process (note: many materials are available for ALD[15]). As a proof of concept, we prepared self-supported carbon coated TiN (notated as: C-TiN) nanotube arrays because recently metal nitrides received numerous interests in the field of electrochemical energy storage.[16] The C-TiN electrode was tested as a negative electrode for aqueous supercapacitor applications. Importantly, we could demonstrate that the long-term cycling ability of C-TiN compared to bare TiN nanotube arrays is strongly improved due to the functional carbon coating, which is, to our knowledge, a key challenge for metal nitride materials in electrochemical energy storage.[17] We believe that this technique could further be beneficial to many other material systems and applications because of the versatility of this approach.

2. Experimental

Synthesis of AAO template: The AAO templates were synthesized from high purity aluminum foils by a two-step anodization process at 40 V in 0.3 M oxalic acid with a 6 h first and 10 – 15 min second anodization time.[11, 18-21] The AAO pores were widened in a 5 wt. % H_3PO_4 solution for 15 min at 30 °C.

Synthesis of micelle: First, a low molecular weight phenolic resol was prepared similar to the method described by Gu et. al[22] by mixing 1.4 mL formaldehyde (37 wt. %), 0.4 g phenol and 10 mL 0.1 M NaOH for 45 min at 70 °C. After that, 10 ml H_2O containing 640 mg of pluronic F-127 were added to the solution and stirred for 120 min at 70 °C. The solution was diluted by adding 35 ml H_2O and then further stirred for 20 h. The color of the solution changed gradually from transparent to Bordeaux red during this process.

AAO coating and carbonization: 3 ml of the prepared micelles solution were added into a 30 ml Teflon based autoclave and 2-3 AAO templates were immersed into the solution and kept still for 120 min. Afterwards, 26 ml H_2O were added, the autoclave was tightly sealed and placed into an oven for 20 h at 130 °C. After the hydrothermal process all AAO templates were cleaned with H_2O and tissue paper until the AAO templates shimmered slightly yellow. Then, the as-modified AAO templates were annealed at 550 °C for 2 h in N_2 atmosphere (3 °C min^{-1} ramp rate) to obtain conformally carbon coated AAO templates.

ALD fabrication of C-TiN and TiN nanotube arrays: C-TiN and TiN nanotube arrays were fabricated from carbon coated and bare AAO templates, respectively. The AAO templates were placed into a *Picosun Sunale R-150* ALD reactor, the temperature was increased to 400 °C and the chamber pressure was decreased to 10 hPa. $TiCl_4$ and NH_3 were used as precursors with respective pulse/purge times of 0.1 s/6 s and 1 s/10 s and a carrier gas flow of 120 sccm. This ALD cycle was repeated for 500 times. Finally, the AAO template was dissolved in a 5 wt. % NaOH solution to gain self-supported C-TiN and TiN nanotube arrays. The active electrode mass was determined by a *Mettler-Toledo XP2 microgram balance* (accuracy 0.1 µg) to ca. 0.12 mg cm^{-2}.

Characterization: All electrochemical measurements were performed in a three electrode cell with a 1 M KOH electrolyte (unless otherwise indicated), double-junction Ag/AgCl reference electrode (3 M KCl) and Pt foil as the counter electrode. The CV and charge/discharge curves were measured from -1.0 – 0 V vs Ag/AgCl at scan rates of 2, 5, 10, 20, 50 and 100 mV s^{-1} and current densities of 1, 2, 5, 10, 25 and 50 A g^{-1}, respectively. All measurements were performed on a *Bio-Logic VSP* electrochemical work station.

The structural characterization was carried out on a SEM (*Hitachi S-4800*) and TEM (*Zeiss Libra 200 FE*) and the X-ray diffraction measurement was performed on a *Siemens D5000* diffractometer.

3. Results and discussion

3.1 Fabrication process and structural investigation

The fabrication of C-TiN and TiN nanotube arrays is realized by a template assisted fabrication process (Figure 1). Thereby C-TiN (route A) and TiN (route B) nanotubes can be synthesized individually in the pores of nano-porous AAO templates by a subsequent coating of carbon and TiN. Bare TiN nanotubes are prepared directly in the pores of AAO via a straight forward atomic layer deposition process from $TiCl_4$ and NH_3 at 400 °C and a subsequent liberalization of the TiN nanotube array by etching the template in a 5 wt. % NaOH solution. In contrast, the formation of a highly conformal 3D carbon coating on the TiN nanotube array could only be realized after the implementation of an innovative coating technique, which is based on the self-assembly of polymeric nano-micelles (PNMs). Such PNMs are buildup of amphiphilic molecules and are synthesized from Pluronic F-127 block copolymer (consists of poly(propylene oxide) and poly(ethylene oxide)) and a phenol/formaldehyde resol.[22] Thereby, PNMs assemble spontaneously in aqueous media due to aggregation of the amphiphilic molecules in which the hydrophilic ends form an outer shell and the hydrophobic ends arrange in the micellar core.[23] The synthesized PNMs serve as fundamental substructures and can self-assemble on the pore walls of an AAO template. A subsequent hydrothermal treatment at 130 °C leads to an interconnection of the assembled PNMs and hence, a 3D conformal coating of the AAO template by a Bakelite resin polymer (yellow in color, Figure 2b). Finally, the as-coated AAO template is tempered at 550 °C in N_2 atmosphere and the polymeric coating is carbonized into a continuous carbon film (black in color, Figure 2c), which covers the entire AAO template. SEM images of the liberated 3D carbon structure (*i.e.*, self-supported carbon nanotubes) and the carbon coated AAO template are displayed and compared to an uncoated AAO template in Figure S1. The images outline that the nano-porous hexagonal AAO morphology is maintained after the carbon

coating process and hence, prove the well conformal coating (each AAO pore of ca. 10^{10} pores cm^{-2} is coated). The TEM investigation of a single carbon nanotube structure, as presented in Figure 2d, shows that the tube diameter of ca. 60 nm is inherited from the AAO template. The subsequent atomic layer deposition of TiN into a carbon coated AAO template leads to the formation of carbon encapsulated TiN, defining the carbon coated TiN morphology. A self-supported C-TiN nanotube array is gained after etching the AAO template in a 5 wt. % NaOH solution. The crystal structure of the ALD prepared TiN is investigated by X-ray diffraction measurements and could be attributed to polycrystalline cubic TiN on the basis of the (111), (200), (220) and (311) crystal planes, as shown in Figure S2. Figure 2e and f display a large magnification and a cross-section SEM image of the as-prepared C-TiN nanotube array (diameter ca. 60 nm, length ca. 1.2 μm), showing the curved close-end nanotube nature (originating from the AAO barrier layer), the self-supporting capacity and the vertical alignment of adjacent nanotubes. The formation of C-TiN nanotubes and the material distribution across the nano-tubular structure is further verified by TEM and EDX line-scans. Figure 2g presents the Ti K_α, N K_α and C K_α line scan profiles which are recorded across a single C-TiN nanotube (1000 ALD cycles for better EDX signal). The spectra show enhanced signal peaks of Ti K_α and N K_α located at the wall positions of the TiN nanotube, proving the hollow nano-tubular nature of TiN. The C K_α spectrum indicates a slightly increased carbon signal across the nanotube which originates from the carbon shell. The thickness of the carbon shell on the TiN nanotube is in the range of ca. 2 - 3 nm and the thickness of the TiN nanotube after 500 ALD cycles is about 10 nm, as indicated in Figure S3. Noteworthy, conformally coated self-supported C-TiN nanotube arrays could not be realized by first synthesizing the TiN nanotube array via route A and the subsequent coating of carbon. This inversed process (compared to route B) is leading to an

overgrowth and results in the formation of a thick carbon film on top of the dense nanotube array, as shown in Figure S4. The reason for the non-conformal coating is based on the fact that excessive amounts of the hydrothermally formed polymer on top and in-between the TiN nanotubes cannot be removed without destroying the nanostructured array and hence will transform during the carbonization step into a carbon layer that is of non-conformal manner. In contrast excessive amounts of formed polymer can easily wiped of the AAO surface, leaving a slightly yellow shimmered template, as shown in Figure 2b. This effect indicates that commonly used carbon coating techniques (*i.e.*, developed for powder samples) cannot directly be applied to dense arrays of self-supported nanostructures. Hence, the successful development of a carbon coating technique that is capable of first fabricating the functional carbon shell and then depositing the active material inside is a breakthrough in synthesizing well conformal functional coatings on self-supported nanostructure arrays.

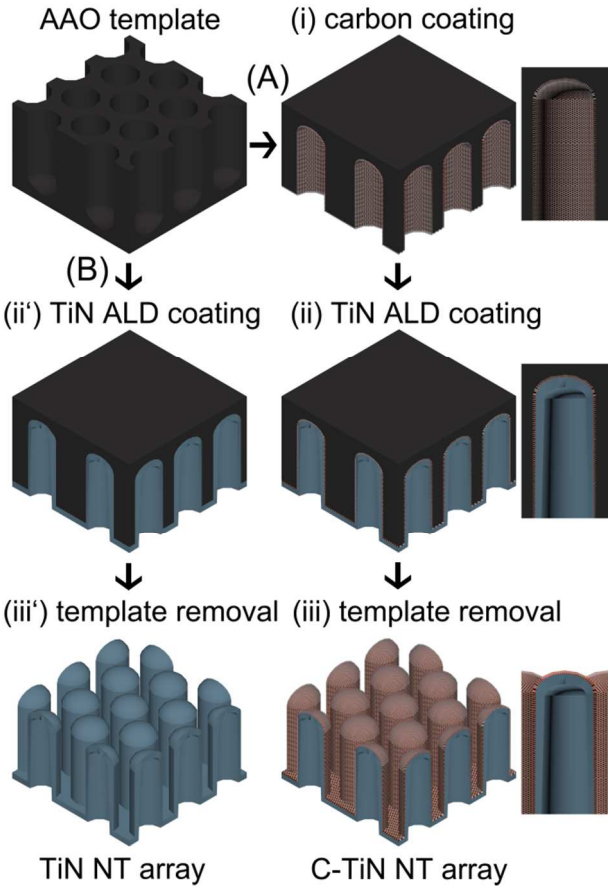

Figure 1. Schematic diagram, illustrating the template-assisted fabrication process of self-supported C-TiN (route A) and TiN (route B) nanotube arrays. Route A: First, a carbon layer is synthesized on the AAO template from self-assembled PNMs and a subsequent annealing process. Then, TiN is deposited by ALD into the carbon coated AAO template; Route B: TiN is directly deposited into an AAO template by ALD.

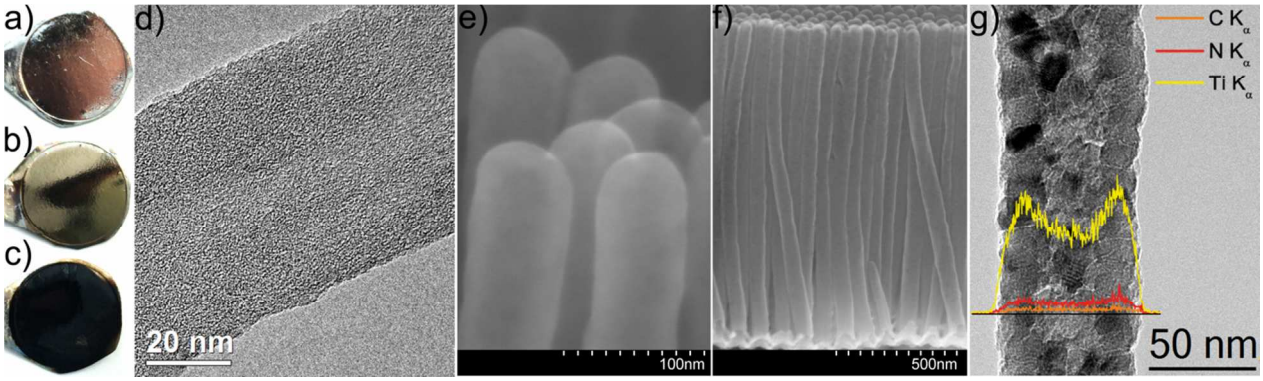

Figure 2. a-c) Pictures of a bare, polymer coated and carbon coated AAO template, respectively; d) TEM image of a single carbon nanotube with a diameter of ca. 60 nm; e, f) large magnification and cross-section SEM images of a C-TiN nanotube array; g) TEM and EDX line-scan of a single C-TiN nanotube.

3.2 Electrochemical performance

The C-TiN and TiN nanotube arrays are both tested as negative electrode materials for aqueous based supercapacitors. The electrochemical performance is investigated by cyclic voltammetry (CV) and galvanostatic charge/discharge measurements in a three-electrode cell, using a 1 M KOH electrolyte, a double-junction Ag/AgCl reference electrode (3 M KCl), and a Pt foil counter electrode in a potential window ranging from -1 V to 0 V. Figure 3a and S5a display the CV curves recorded for C-TiN and TiN at a variety of scan rates between 2 mV s^{-1} and 100 mV s^{-1}, respectively. The C-TiN nanotube array exhibits, even at high scan rates, a quasi-rectangular CV shape, which indicates well reversible electrochemical charge storage and good capacitive behavior. In comparison, the electrode based on bare TiN nanotubes shows some distortion at high scan rates. This behavior is supported by results obtained from galvanostatic charge/discharge measurements (Figure 3b and S5b), which were performed at current densities ranging from 1 A g^{-1} to 50 A g^{-1}. The C-TiN based electrode shows a more pronounced equilateral triangular shape of the consecutive charging and discharging processes, as expected for electrochemical charge storage in supercapacitors. Whereas the slope of the charging process for bare TiN based electrodes is clearly elongated compared to the discharging process, resulting in an inferior charge/discharge efficiency. On the basis of the constant current discharge curves, the specific capacitances and the rate capabilities (Figure 3c) of the C-TiN and TiN nanotube arrays are calculated, according to the following equation:

$$c = \mathrm{I}/(\frac{\Delta V}{\Delta t} \times m) \quad (2)$$

with c (F g^{-1}), I (A), $\frac{\Delta V}{\Delta t}$ (V s^{-1}) and m (g) being the specific capacitance, discharge current, gradient of discharge curve obtained by dividing the width of the potential window (*i.e.*, 1 V) by the discharge time, and mass of the active material, respectively. The C-TiN nanotube array exhibits a specific capacitance of 167 F g^{-1} at 1 A g^{-1} and remains 95 F g^{-1} at 50 A g^{-1}. While the TiN nanotube array possesses 140 F g^{-1} at 1 A g^{-1} and remains 61 F g^{-1} at 50 A g^{-1}. The performance enhancement of the C-TiN over the TiN nanotube array at low current density can most likely be attributed to the active carbon shell, which itself contribute about 9.5 % to the specific capacitance, as shown in Figure S6. Whereas the pronounced decrease of specific capacitance at high scan rates most likely originates from the poor cycling stability of the bare TiN electrode (prolonged cell history at high scan rates). Further, investigations of the electrochemical performance of the C-TiN electrode in a neutral electrolyte (1 M Na_2SO_4) have shown that the specific capacitance decreased strongly and could only remain around 30 % of the specific capacitance obtained in the alkaline electrolyte (1 M KOH). With a view on aqueous based asymmetric supercapacitor configurations is TiN therefore a less suitable negative electrode material in systems that operate best in neutral electrolytes, like MnO_2. Moreover, TiN should be considered as a negative electrode material in combination with complementary positive electrode materials like carbon based materials (exhibit high specific capacitance in alkaline electrolytes of up to 250 F g^{-1}),[24] metal hydroxides (*e.g.*, Co(OH)[25] and $Ni(OH)_2$[26]) and metal oxides (*e.g.*, $Ni_{0.3}Co_{2.7}O_4$,[27] NiO[28]). Most importantly, the 3D self-assembled carbon shell can efficiently stabilize the TiN nanotube array during long-term cycling. Figure 3d displays the capacitance retention obtained for C-TiN and TiN nanotube arrays during 6000 consecutive charge/discharge cycles performed at 10 A g^{-1}. As similarly reported by others,[29-32] the bare TiN

based electrode suffered from severe capacitance loss and could only retain about 15 % of its original capacitance after 6000 cycles. In contrast, the carbon coated TiN electrode shows a considerably improved long-term cycling ability and exceeds, with 70 % of the initial capacitance retained after 6000 cycles, the performance of bare TiN by more than 4.5 times. Hence, the performance enhancement can directly be attributed to the carbon shell, which primarily acts as a cage for TiN and prevents a structural breakdown and electrode pulverization during cycling. The SEM images in Figure 4 clearly outline that carbon coated TiN nanotubes can maintain the initial nano-tubular structure even after 6000 consecutive charge/discharge cycles, while uncoated TiN nanotubes undergo a severe change in morphology and devolve into a film like structure.

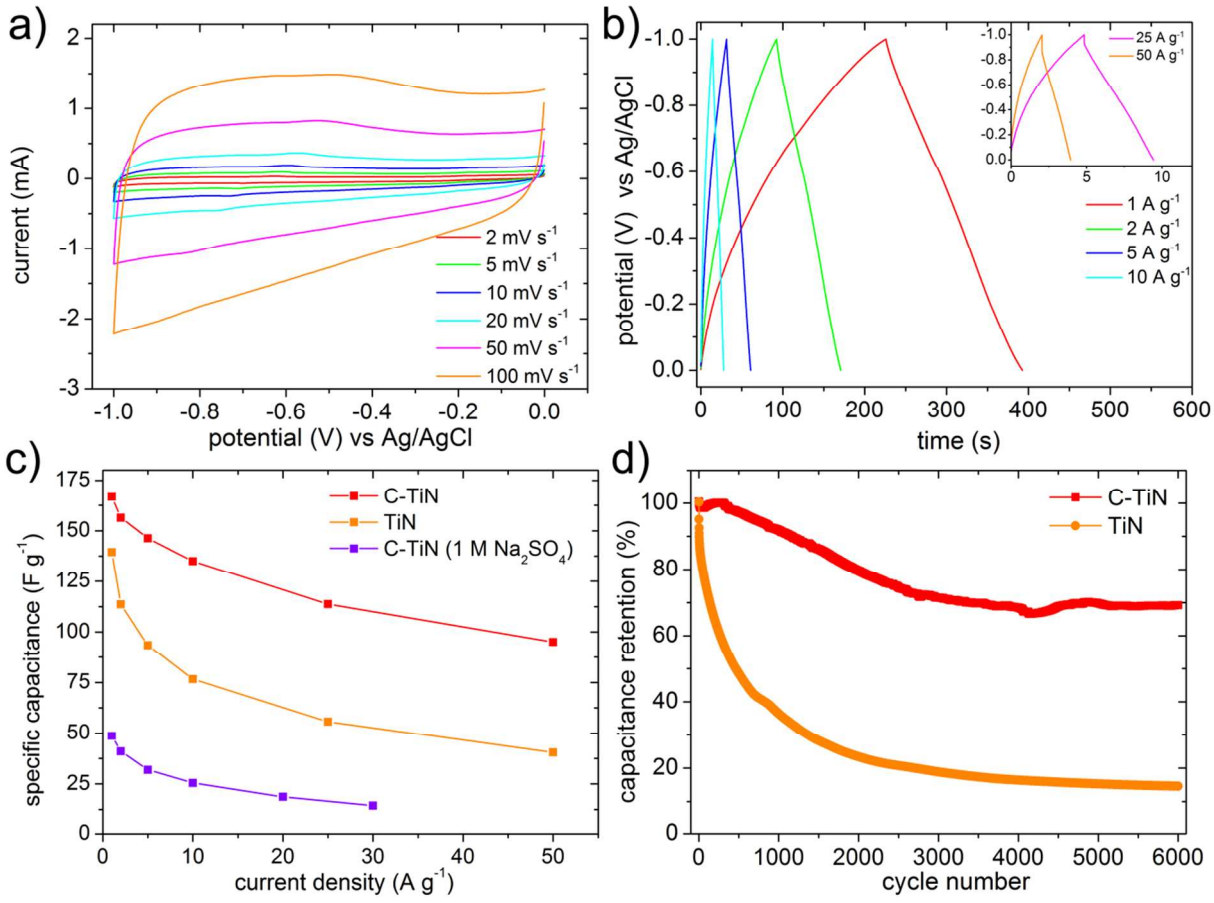

Figure 3. Electrochemical investigation of the C-TiN and TiN nanotube arrays measured in a three-electrode configuration. a, b) CV and charge/discharge profiles of the C-TiN nanotube array; c) Rate performance of the C-TiN (in 1 M KOH and 1 M Na_2SO_4 electrolyte) and bare TiN (1 M KOH); d) Long-term cycling ability of the C-TiN and TiN nanotube arrays.

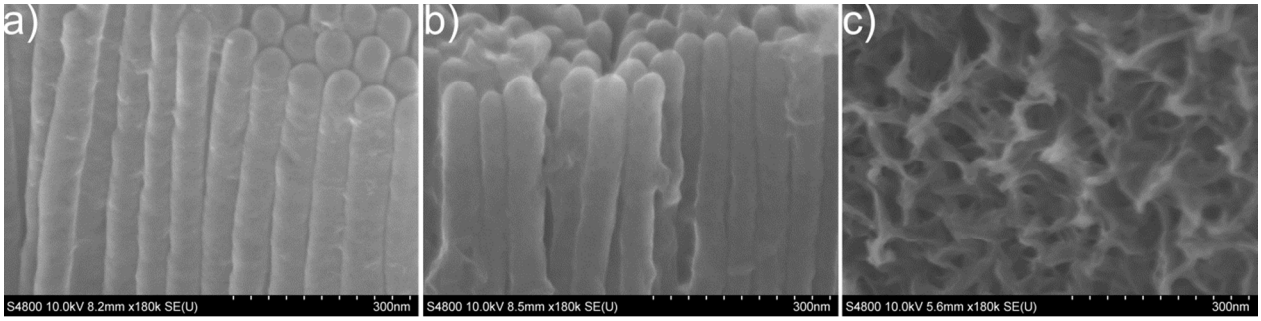

Figure 4. Morphology investigation of the C-TiN and TiN electrode before and after long-term cycling. a) C-TiN nanotube array before cycling; b) Preserved C-TiN nanotube structure after 6000 charge/discharge cycles; c) Initial TiN nanotube array has devolved into a film like structure after 6000 charge/discharge cycles.

4. Conclusion

In summary, this work describes an innovative approach to synthesize carbon coatings on dense self-supported nanostructure arrays. As a proof of concept, C-TiN nanotube arrays, which can serve as a negative electrode material for aqueous based supercapacitors, were synthesized. Importantly, it could be shown that the C-TiN exhibits a superior long-term cycling ability compared to bare TiN nanotube arrays. Considering the fact that many of the challenges that face the field of aqueous supercapacitors are related to difficulties associated with high-voltage asymmetric device configurations and long-term cycling ability, the fabrication of stable C-TiN nanotube arrays as an alternative choice for a negative electrode material could accelerate the

progress in this field and lead to energy storage devices that are safe to operate and have limited environmental impact. Noteworthy, the developed carbon coating technique is not limited to TiN and could most likely enhance the performance of other active materials in a wide range of applications.

Acknowledgment

This work was financially supported by European Research Council (ThreeDsurface: 240144), BMBF (ZIK-3DNanoDevice: 03Z1MN11), BMBF (Meta-ZIK-BioLithoMorphie: 03Z1M511), and Volkswagen-Stiftung (Herstellung funktionaler Oberflächen: I/83 984). We kindly acknowledge the help of Nina Winkler (University of Münster) for supplying TEM measurements.

References

1. J. Deng, X. Lv, J. Gao, A. Pu, M. Li, X. Sun and J. Zhong, *Energy Environ. Sci.*, 2013, **6**, 1965-1970.
2. H. Li and H. Zhou, *Chem. Commun.*, 2012, **48**, 1201-1217.
3. F. Cheng, J. Liang, Z. Tao and J. Chen, *Adv. Mater.*, 2011, **23**, 1695-1715.
4. X. Lu, T. Liu, T. Zhai, G. Wang, M. Yu, S. Xie, Y. Ling, C. Liang, Y. Tong and Y. Li, *Adv. Energy Mater.*, 2014, , DOI: 10.1002/aenm.201300994.
5. Y. Gogotsi, in *Nanostructured Films and Coatings*, eds. G.-M. Chow, I. Ovid'ko and T. Tsakalakos, Springer Netherlands, 2000, p. 32.
6. J. W. Long, B. Dunn, D. R. Rolison and H. S. White, *Chem. Rev.*, 2004, **104**, 4463-4492.
7. T. S. Arthur, D. J. Bates, N. Cirigliano, D. C. Johnson, P. Malati, J. M. Mosby, E. Perre, M. T. Rawls, A. L. Prieto and B. Dunn, *MRS Bull.*, 2011, **36**, 523-531.
8. D. R. Rolison, J. W. Long, J. C. Lytle, A. E. Fischer, C. P. Rhodes, T. M. McEvoy, M. E. Bourg and A. M. Lubers, *Chem. Soc. Rev..*, 2009, **38**, 226-252.
9. A. Kargar, K. Sun, Y. Jing, C. Choi, H. Jeong, G. Y. Jung, S. Jin and D. Wang, *ACS Nano*, 2013, **7**, 9407-9415.
10. Y. J. Hwang, A. Boukai and P. Yang, *Nano Lett.*, 2008, **9**, 410-415.
11. Y. Lei, W. Cai and G. Wilde, *Prog. Mater. Sci.*, 2007, **52**, 465-539.
12. F. Grote, L. Wen and Y. Lei, *J. Power Sources*, 2014, **256**, 37-42.
13. F. Grote, R.-S. Kühnel, A. Balducci and Y. Lei, *Appl. Phys. Lett.*, 2014, **104**, 053904

14. S. R. Gowda, A. Leela Mohana Reddy, X. Zhan and P. M. Ajayan, *Nano Lett.*, 2011, **11**, 3329-3333.
15. Ultratech/CambridgeNanotech, www.cambridgenanotech.com/periodic.
16. S. Dong, X. Chen, X. Zhang and G. Cui, *Coord. Chem. Rev.*, 2013, **257**, 1946-1956.
17. R. L. Porto, R. Frappier, J. B. Ducros, C. Aucher, H. Mosqueda, S. Chenu, B. Chavillon, F. Tessier, F. Cheviré and T. Brousse, *Electrochim. Acta*, 2012, **82**, 257-262.
18. H. Masuda and K. Fukuda, *Science*, 1995, **268**, 1466-1468.
19. M. Wu, L. Wen, Y. Lei, S. Ostendorp, K. Chen and G. Wilde, *Small*, 2010, **6**, 695-699.
20. Y. Lei, W.-K. Chim, Z. Zhang, T. Zhou, L. Zhang, G. Meng and F. Phillipp, *Chem. Phys. Lett.*, 2003, **380**, 313-318.
21. Z. Chen, Y. Lei, H. G. Chew, L. W. Teo, W. K. Choi and W. K. Chim, *J. Crys. Growth*, 2004, **268**, 560-563.
22. D. Gu, H. Bongard, Y. Meng, K. Miyasaka, O. Terasaki, F. Zhang, Y. Deng, Z. Wu, D. Feng, Y. Fang, B. Tu, F. Schüth and D. Zhao, *Chem. Mater.*, 2010, **22**, 4828-4833.
23. K. Letchford and H. Burt, *Eur. J. Pharm. Biopharm.*, 2007, **65**, 259-269.
24. J. W. Long, D. Bélanger, T. Brousse, W. Sugimoto, M. B. Sassin and O. Crosnier, *MRS Bull.*, 2011, **36**, 513-522.
25. S. Gao, Y. Sun, F. Lei, L. Liang, J. Liu, W. Bi, B. Pan and Y. Xie, *Angew. Chem. Int. Ed.*, 2014, DOI: 10.1002/anie.201407836.
26. H. B. Li, M. H. Yu, F. X. Wang, P. Liu, Y. Liang, J. Xiao, C. X. Wang, Y. X. Tong and G. W. Yang, *Nat. Commun.*, 2013, **4**, 1894.
27. H. B. Wu, H. Pang and X. W. Lou, *Energy Environ. Sci.*, 2013, **6**, 3619-3626.
28. E. Eustache, R. Frappier, R. L. Porto, S. Bouhtiyya, J.-F. Pierson and T. Brousse, *Electrochem. Commun.*, 2013, **28**, 104-106.
29. X. Lu, G. Wang, T. Zhai, M. Yu, S. Xie, Y. Ling, C. Liang, Y. Tong and Y. Li, *Nano Lett.*, 2012, **12**, 5376-5381.
30. D. Choi and P. N. Kumta, *J. Electrochem. Soc.*, 2006, **153**, A2298-A2303.
31. X. H. Zhou, C. Q. Shang, L. Gu, S. M. Dong, X. Chen, P. X. Han, L. F. Li, J. H. Yao, Z. H. Liu, H. X. Xu, Y. W. Zhu and G. L. Cui, *ACS App. Mater. Interfaces*, 2011, **3**, 3058-3063.
32. S. Dong, X. Chen, L. Gu, X. Zhou, H. Wang, Z. Liu, P. Han, J. Yao, L. Wang, G. Cui and L. Chen, *Mater. Res. Bull.*, 2011, **46**, 835-839.

TOC Figure and TOC entry

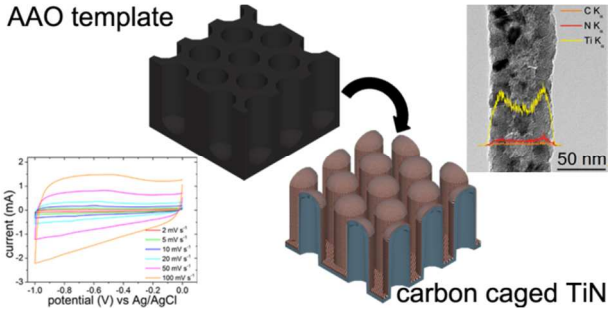

Innovative carbon coating on nano-porous anodic aluminum oxide templates enables coatings on dense self-supported nanostructured arrays in a reversed manner for applications in energy devices (*e.g.*, supercapacitors)